Molecular Biology of the Cell
Vol. 12, 831–845, April 2001

Inhibition of Endothelial Wound Repair by Dominant Negative Connexin Inhibitors

Brenda R. Kwak,*† Michael S. Pepper,* Daniel B. Gros,‡ and Paolo Meda*

*Department of Morphology, University of Geneva Medical Center, Switzerland; and ‡LGPD-IBDM, Campus de Luminy, 13288 Marseille, France

Submitted December 27, 1999; Revised December 18, 2000; Accepted January 30, 2001
Monitoring Editor: Joan Brugge

Wounding of endothelial cells is associated with altered direct intercellular communication. To determine whether gap junctional communication participates to the wound repair process, we have compared connexin (Cx) expression, cell-to-cell coupling and kinetics of wound repair in monolayer cultures of PymT-transformed mouse endothelial cells (clone bEnd.3) and in bEnd.3 cells expressing different dominant negative Cx inhibitors. In parental bEnd.3 cells, mechanical wounding increased expression of Cx43 and decreased expression of Cx37 at the site of injury, whereas Cx40 expression was unaffected. These wound-induced changes in Cx expression were associated with functional changes in cell-to-cell coupling, as assessed with different fluorescent tracers. Stable transfection with cDNAs encoding for the chimeric connexin 3243H7 or the fusion protein Cx43-βGal resulted in perturbed gap junctional communication between bEnd.3 cells under both basal and wounded conditions. The time required for complete repair of a defined wound within a confluent monolayer was increased by ~50% in cells expressing the dominant negative Cx inhibitors, whereas other cell properties, such as proliferation rate, migration of single cells, cyst formation and extracellular proteolytic activity, were unaltered. These findings demonstrate that proper Cx expression is required for coordinated migration during repair of an endothelial wound.

INTRODUCTION

The vascular endothelium consists of a continuous quiescent monolayer of cells lining the luminal surface of the entire vascular system, which provides a structural and metabolic barrier between blood and underlying tissues. Endothelial cells are induced to migrate during the process of new capillary blood vessel formation and during repair of the endothelial lining after injury in large vessels. Although endothelial cells migrate as tube-like sprouts from preexisting vessels during angiogenesis (Risau, 1991), wound repair in large vessels is characterized by migration of a sheet of endothelial cells (Schwartz *et al.*, 1978). Intercellular communication between endothelial cells has been suggested to play a role in coordinating the migration process (Larson and Haudenschild, 1988; Pepper *et al.*, 1989).

One type of direct cell-to-cell communication is provided by gap junction channels. The connexins (Cx) proteins comprising these channels, form a multigene family consisting of at least 15 members in mammals (White and Paul, 1999). Each connexin forms channels with different properties of gating, permeability, and selective interaction with other connexins (Bruzzone *et al.*, 1996; Kumar and Gilula, 1996). In situ, endothelial gap junctions consist of Cx43, Cx40, and Cx37, depending on the type of vessel and its position in the vascular tree (Larson *et al.*, 1990; Bastide *et al.*, 1993; Bruzzone *et al.*, 1993; Reed *et al.*, 1993; Blackburn *et al.*, 1995; Little *et al.*, 1995a; VanRijen *et al.*, 1997; Yeh *et al.*, 1997). Although Cx40 and Cx37 are widely distributed within the vascular endothelium, Cx43 shows a more heterogeneous expression pattern (Gabriels and Paul, 1998). Expression levels of Cx43 are higher in large arteries of the vascular tree (Hong and Hill, 1998) and at regions that experience disturbed blood flow (Gabriels and Paul, 1998).

Intercellular communication, as assessed by diffusion of fluorescent dyes, has been demonstrated in both large vessel and microvascular endothelial cells (Larson and Sheridan, 1982; Larson *et al.*, 1987; Larson and Haudenschild, 1988; Pepper *et al.*, 1989, 1992; Pepper and Meda, 1992; Little *et al.*, 1995b). Microvascular endothelial cells migrating from the edges of a mechanically induced wound display increased junctional coupling relative to cells distant from the wound (Pepper *et al.*, 1989). This wound-induced increase in coupling is accompanied by an increase in Cx43 mRNA and protein (Pepper *et al.*, 1992), suggesting that this connexin may play an important role during wound repair. For sheet migration of large vessel endothelial cells, on the other hand,

† Corresponding author. E-mail address: brendakwak@hotmail.com.
† Present address: University Hospital Geneva, Division of Cardiology, 1211 Geneva, Switzerland.

junctional coupling and/or Cx43 expression levels have been reported to be slightly decreased, unaltered, or even increased in a similar experimental system (Larson and Haudenschild, 1988; Pepper *et al.*, 1992; Gabriels and Paul, 1993). Hence, the effect of wounding on junctional communication may depend on a variety of factors, including the origin of endothelial cells and the connexin types expressed.

Pharmacological blockade of gap junctional communication has been used previously to explore the relationship between cell coupling and migration (Pepper *et al.*, 1989). These studies, however, do not provide information on the contribution of different endothelial connexins involved in wound repair. To this end, we have used PymT-transformed mouse endothelial cells expressing the three native endothelial connexins and transfected these cells with cDNAs coding for two different dominant negative connexin inhibitors. Although the chimeric connexin 3243H7 (Paul *et al.*, 1995) and the fusion protein Cx43-βGal (Sullivan and Lo, 1995) showed different subcellular localizations, both strongly altered connexin expression and the pattern of intercellular communication between bEnd.3 cells. Both dominant negative inhibitors also significantly inhibited the rate of endothelial wound repair, whereas proliferation rate, migration of single cells, cyst formation, and extracellular proteolytic activity were unaffected. Taken together, these data demonstrate that direct intercellular communication serves to coordinate migration during repair of the endothelial lining.

MATERIALS AND METHODS

Cell Culture and Transfection

bEnd.3 cells (Montesano *et al.*, 1990) were maintained in DMEM supplemented with 10% fetal calf serum, 50 IU/ml penicillin, and 50 μg/ml streptomycin, hereafter referred to as complete culture medium. Cells were transfected with 20 μg of either pEFZ (kindly provided by Dr. C. W. Lo, University of Pennsylvania, Philadelphia, PA) or p3243H7Et (kindly provided by Dr. D. L. Paul, Harvard Medical School, Boston, MA) and 2 μg of a plasmid containing the gene for hygromycin resistance (Blochlinger and Dingelmann, 1984). Parallel cultures were transfected with 20 μg of the latter plasmid alone. pEFZ is an expression vector that encodes the full-length mouse Cx43 polypeptide fused at its COOH terminus to bacterial β-galactosidase. p3243H7Et is an expression vector that encodes a 12CA5 epitope-tagged chimeric polypeptide composed of fused portions of rat Cx32 and Cx43. Both the fusion and the chimeric protein have been shown to exhibit dominant negative inhibitory activity on gap junction channels (Paul *et al.*, 1995; Sullivan and Lo, 1995). Transfection was performed using the electroporation technique (parameters: 250 or 300 V, 21–23 s, 960 μF). Two days after transfection, cells were subjected to hygromycin selection (200 U hygromycin B/ml; Calbiochem, La Jolla, CA). Resistant cells growing into small colonies were observed after 8–10 days of selection. These cells were trypsinized in clonal rings, grown separately, and subsequently screened for expression of either the fusion protein or the chimeric protein by RT-PCR and immunocytochemistry. Once these clones were established, they were maintained by plating at 5×10^5 cells per 25-cm^2, gelatin-coated culture flask and passaged every 3–4 days.

Human cervical carcinoma HeLa cells transfected with cDNAs encoding for murine Cx37, Cx40, or Cx43 were kindly provided by Dr. K. Willecke (University of Bonn, Germany). They were maintained in complete culture medium supplemented with 2 mM L-glutamine, and 1 mg/ml G418 (for Cx43 transfectants) or 0.5 μg/ml puromycin (for Cx40 and Cx37 transfectants).

Wound Repair

Cells were seeded into 35-mm gelatin-coated culture dishes at $1–2 \times 10^5$ cells/dish and grown to confluence in complete culture medium (2–3 days). At confluence, the monolayers were mechanically wounded with a 6-mm-wide rubber policeman, detached cells were removed, and fresh complete medium was added. Wounded monolayers were incubated at 37°C in an air/CO_2 (97%:3%) atmosphere and culture medium was replaced every 3–4 days. The distance between the two wound edges was determined using an inverted phase contrast microscope (Nikon, Tokyo, Japan) every 24 h until the wound was completely closed. Results are expressed as mean ± SEM and compared using an independent Student's *t* test.

Determination of Gap Junctional Communication

Cells were seeded at $1–2 \times 10^5$ cells/35-mm, gelatin-coated culture dish and grown in complete culture medium. Cell-to-cell coupling was determined 2 days later in subconfluent monolayers by microinjection (see below). Coupling was also studied 24 h after wounding by two complementary approaches. In the first, wounded monolayers were scrape-loaded with a mixture of Lucifer Yellow (Sigma, St. Louis, MO) and dextran rhodamine (Molecular Probes, Eugene, OR) or with propidium iodide (Sigma), according to the technique described by El-Fouly *et al.* (1987). In the second approach, cells were microinjected with Lucifer Yellow (Stewart, 1978).

For scrape-loading, monolayers were rinsed with PBS, and incubated in 1 ml PBS containing 2% Lucifer Yellow and a few crystals of 10,000-mol wt dextran-tetramethylrhodamine. The monolayers were then scraped perpendicular to the original endothelial wound using a mini–glass cutter and incubated in the dark for 3 min at room temperature. The Lucifer Yellow-dextran rhodamine mixture was then removed, and the cultures were washed several times with PBS and fixed in 4% paraformaldehyde in 0.1 M phosphate buffer (pH 7.4). A similar procedure was followed for scrape-loading with propidium iodide (5 mg/ml in PBS). Scrape-loaded cultures were photographed under both phase-contrast and fluorescence illumination. Fluorescent cells were scored in five experiments. The number of cells per 100 μm of scrape length is expressed as mean ± SEM.

For microinjection, subconfluent or wounded cultures were rinsed with a control solution containing 130 mM NaCl, 4 mM KCl, 1.8 mM $CaCl_2$, 0.56 mM $MgCl_2$, 10 mM glucose, 1.2 mM NaH_2PO_4, 14.3 mM HEPES (pH 7.4) and transferred to the stage of an inverted microscope (Nikon Diaphot TMD). Individual endothelial cells were impaled at room temperature with microelectrodes filled with a 4% Lucifer Yellow solution prepared in 150 mM LiCl and buffered to pH 7.2 with 10 mM HEPES. The fluorescent tracer was allowed to fill the cells by simple diffusion for 3 or 5 min in wounded or subconfluent cultures, respectively. For wounded cultures, microinjections were performed both at the edge of the endothelial wound and at distance from it. The first region, called "wound," comprised ~8 cell rows from the wound edge. The second region, called "outside the wound," was separated from the first by at least 30 cell rows. After the injection period, the electrode was removed, and the number of fluorescent cells was counted. Experiments were performed at room temperature. Cells were visualized using epifluorescent illumination provided by a 100 W mercury lamp and appropriate filters. Results are expressed as mean ± SEM. Dye coupling under different conditions was compared using an independent Student's *t* test.

RNA Isolation and RT-PCR

mRNA was isolated from bEnd.3 cell clones using oligo(dT) columns (Pharmacia Biotechnology, Uppsala, Sweden), according to the manufacturer's instructions. Reverse transcription (RT) was carried out using random hexamers, and the resulting cDNA was amplified by PCR, using the following primer pairs: for Cx43: sense, 5′-CGGCGGCTTCACTTTCATTA-3′ and antisense, 5′-AGAACACATGGGCCAAG-

TAC-3′; for 3243H7: sense, 5′-TCCGGCATCTGCATTATCCTC-3′ and antisense, 5′-TGGCTAATGGCTGGAGTTCAT-3′; for Cx43-βGal: sense, 5′-CCCCACTCTCACCTATGTCTCC-3′ and antisense, 5′-TGGGTAACGCCAGGGTTTTCCC-3′.

After a 5 min start at 94°C, amplification of cDNA was carried out for 30 cycles, each comprising 1 min at 94°C, 1 min at 58°C, and 2 min at 72°C, using a DNA Thermal Cycler 480 (Perkin Elmer-Cetus, Norwalk, CT). After the last cycle, an elongation step of 5 min at 72°C was performed. Amplified DNA fragments were separated in parallel with molecular weight markers (100-bp DNA Ladder; Life Technologies, Grand Island, NY) in a 2% agarose gel and stained with ethidium bromide.

Antibodies

Polyclonal antibodies raised in rabbits against oligopeptides of the carboxy-terminus of Cx40, amino acids 335–356 (Gros *et al.*, 1994); Cx37, amino acids 315–331 (Delorme *et al.*, 1997; VanRijen *et al.*, 1997); C37, amino acids 229–333 (Goliger and Paul, 1994); and Cx37, amino acids 266–281 (Haefliger *et al.*, 2000) were used. Rabbit polyclonal antibodies raised against Cx43 and β-galactosidase were purchased from Zymed Laboratories (South San Francisco, CA) and Cappel Laboratories (Malvern, PA), respectively. A mouse monoclonal antibody recognizing the 12CA5 epitope (anti-HA) was purchased from Boehringer Mannheim (Mannheim, Germany).

Immunofluorescence

For immunofluorescence labeling, cells were cultured on gelatin-coated, 18 × 18-mm glass coverslips in complete culture medium. Confluent monolayers were mechanically wounded with a 6-mm-wide rubber policeman, detached cells were removed, and fresh complete medium was added. Wounded monolayers were incubated thereafter at 37°C in an air/CO_2 (97%:3%) atmosphere and 24 h later fixed for 5 min with methanol at −20°C. The coverslips were rinsed and incubated successively with 0.2% Triton X-100 in PBS for 1 h, 0.5 M NH_4Cl in PBS for 15 min, and in PBS supplemented with 2% bovine serum albumin for another 30 min. Cells were then incubated overnight with primary antibody at appropriate dilutions (for anti-Cx37 3 μg/ml, for anti-Cx40 3 μg/ml, for anti-Cx43 1 μg/ml, for anti-β-galactosidase 1:100 and for anti-HA 1:200) and 10% normal goat serum (Sigma) in PBS. After rinsing, the coverslips were incubated with secondary antibodies conjugated to FITC for 4 h. All steps were performed at room temperature and in between incubation steps cells were rinsed with PBS. Coverslips were mounted on slides in paraphenylenediamineglycerine. Cells were examined using a Zeiss Axiophot microscope (Oberkochen, Germany) equipped with appropriate filters. Specificity of the immunolabeling was checked for by replacing the primary antibody with preimmune serum (anti-Cx40 and anti-Cx37) or by PBS (all other antibodies).

Western Blotting and Immunoprecipitation

Cells were seeded into 100-mm, gelatin-coated culture dishes at 6 × 10^5 cells/dish and grown to confluence in complete culture medium (2–3 days). Multiple wounding experiments were performed as follows: 30 parallel wounds were created in a confluent monolayer with a 2-mm-wide rubber policeman, the dish was rotated through 90°, and an additional 30 parallel wounds were created perpendicular to the first set. Culture medium and detached cells were removed, and fresh complete medium was added. Medium was similarly changed in nonwounded cultures, which were used in parallel as controls. Twenty-four hours later, cells were rinsed with cold PBS, scraped into an ice-cold solubilization buffer consisting of 50 mM Tris-HCl (pH 7.4), 150 mM NaCl, 1% sodium deoxycholate, 1% Nodinet-P40, 0.1% sodium dodecylsulfate, 2.5 mM sodium orthovanadate, 125 mM phenylarsine oxide, and 2 mM phenylmethyl sulfonyl fluoride, and stored at −80°C. After thawing, the samples were centrifuged for 30 min at 13,000 × *g* and 4°C. Supernatants containing solubilized material were recovered, and total amounts of protein were quantified using a bicinchoninic acid quantification assay (Sigma).

Table 1. Dye coupling is inhibited in monolayers and cysts of bEnd.3 cells expressing dominant negative Cx

Clone	Group	Cell-to-cell coupling	SEM	Number of injections
Monolayers[a]				
bEnd.3	Control	9.1	0.6	15
A3	Hygromycin	9.2	0.5	10
B3	3243H7	4.0[b]	0.5	10
B5	3243H7	2.4[b]	0.4	10
D1	Cx43-βGal	3.9[b]	0.6	10
D2	Cx43-βGal	2.3[b]	0.6	10
Cysts[c]				
bEnd.3	Control	8.0	0.7	4
B5	3243H7	2.0[d]	0.5	5
D2	Cx43-βGal	1.8[d]	0.3	4

[a] The number of cells labeled with Lucifer Yellow after a 5 min microinjection was determined in subconfluent monolayer cultures of the parental bEnd.3 cell line, a clone transfected with the hygromycin resistance gene only (A3), two independent clones of bEnd.3 cells transfected with either 3243H7 cDNA (B3 and B5) or Cx43βGal cDNA (D1 and D2).

[b] Dye coupling of clones B3, B5, D1, and D2 was significantly different ($p < 0.01$) from that of both bEnd.3 and A3 cells.

[c] The number of cells labeled with Lucifer Yellow after a 5-min microinjection was determined in cysts grown of the parental bEnd.3 cells, clone B5, or clone D2.

[d] Dye coupling in cysts of clones B5 and D2 was significantly different ($p < 0.01$) from that in cysts formed by bEnd.3 cells.

Fifty micrograms (for Cx37), 25 μg (for Cx40), or 15 μg (for Cx43) of protein was loaded on 12% SDS-polyacrylamide gel, electrophoresed, and electrotransferred onto nitrocellulose membranes (Bio-Rad, Hercules, CA). Membranes were then soaked overnight at 4°C in a 2% defatted milk saturation buffer consisting of 10 mM Tris-HCl (pH 7.4), 2 mM EDTA, 133 mM NaCl, 0.05% Triton X-100, and 0.2% sodium azide. Blotted proteins were then incubated for 1 h at room temperature with rabbit polyclonal Cx37 (1.5 μg/ml), Cx40 (2 μg/ml), or Cx43 (2 μg/ml) antibodies. This was followed by a 1-h incubation with goat anti-rabbit secondary antibody conjugated to peroxidase (Jackson ImmunoResearch Laboratories, West Grove, PA). Immunoreactivity was detected using the ECL chemiluminescent detection kit (Amersham, Zurich, Switzerland) according to the manufacturer's instructions. The chemiluminescence reaction was visualized on Biomax ML film (Eastman Kodak, Rochester, NY). Specificity of the Cx43 labeling was confirmed by preabsorption for 15 min at room temperature with its immunogenic peptide (20 μg/ml; Zymed Laboratories). Specificity of the Cx37 or Cx40 labeling was checked by replacing the primary antibody with preimmune serum.

Immunoprecipitation was carried out according to Harlow and Lane (1988) using 50 μg of protein in 0.5 ml lysis buffer, 50 μl anti-HA, and protein G beads (Sigma). The supernatants and precipitated proteins were subjected to Western blotting and detected with Cx43 antibodies as described above.

Determination of Proliferation Rates

Cell proliferation was studied using two complementary approaches. In the first, cells were plated at a density of 5 × 10^5 per

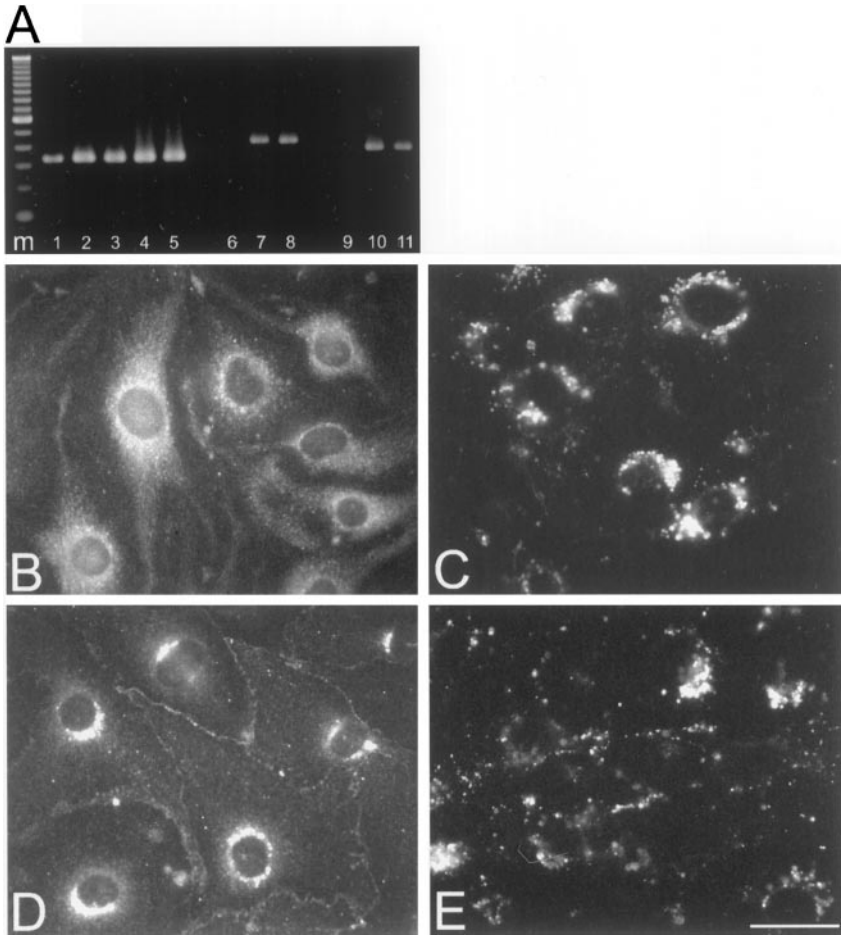

Figure 1. Expression of dominant negative Cx in parental and transfected bEnd.3 cells. (A) mRNA isolated from parental and transfected cells was amplified in a RT-PCR reaction using primer pairs specific for Cx43 (lanes 1–5), 3243H7 (lanes 6–8), or Cx43βGal (lanes 9–11). An aliquot of the PCR amplification reaction was electrophoresed in a 2% agarose gel. Lanes 1, 6, and 9: parental bEnd.3 cells; lanes 2 and 7: bEnd.3/3243H7 cells clone B3; lanes 3 and 8: bEnd.3/3243H7 cells clone B5; lanes 4 and 10: bEnd.3/Cx43βGal cells clone D1; lanes 5 and 11: bEnd.3/Cx43βGal cells clone D2; and lane m:100-bp ladder. (B–E) Subconfluent cultures of bEnd.3/3243H7 and bEnd.3/Cx43βGal cells were incubated with anti-HA and anti-βGalactosidase antibodies, respectively, as well as with anti-Cx43 antibodies. In bEnd.3/3243H7 cells, the chimeric protein (B) was detected predominantly in the perinuclear region, although some diffuse fluorescence was also present throughout the cytoplasm. Note the absence of immunostaining at the sites of cell-to-cell contact. In bEnd.3/Cx43-βGal cells (D), the fusion protein was detected as punctate spots in regions of cell-to-cell contact and in the perinuclear region of the cytoplasm. Similar labeling patterns were observed using Cx43 antibodies (C and E). Bar, 30 μm.

25-cm^2, gelatin-coated culture flask. Every 3–4 days cells were trypsinized, counted with a hemocytometer, and replated at the same density. Total cumulative cell numbers were determined over a 21-d period. In the second approach, cells were seeded on gelatin-coated, 18 $\times$ 18-mm glass coverslips at 1 $\times$ 10^5 cells/coverslip and grown to confluence in complete culture medium (1–2 days). Confluent monolayers were mechanically wounded with a 6-mm-wide rubber policeman, detached cells were removed, and fresh complete medium containing 10 μM bromodeoxyuridine (BrdU; Boehringer Mannheim) was added. Wounded monolayers were incubated 24 h at 37°C in an air/CO_2 (97%:3%) atmosphere and fixed for 5 min with methanol at −20°C. BrdU incorporation was examined by immunostaining with a BrdU antibody (Amersham) according to the manufacturer's directions, after which the cells were counterstained with Evans Blue for determination of total cell numbers. The percentage of BrdU-labeled cells was determined both at the edge of the endothelial wound and at a distance from it. Results of five independent experiments are expressed as mean ± SEM BrdU labeling under different conditions was compared using an independent Student's *t* test.

Time-Lapse Video Imaging

For video imaging, low-density cultures of bEnd.3 cells were rinsed with HEPES-buffered (25 mM) DME supplemented with 10% fetal calf serum, 50 IU/ml penicillin, and 50 μg/ml streptomycin and transferred to the stage of an inverted microscope (Nikon Diaphot TMD). Experiments were performed at 37°C. Images were sampled every 12 s over a period of 8 h using a CCD camera (JVC, Oberwil, Switzerland) and time-lapse VCR (JVC BR-S929E). For analysis, the data were played back on a TV screen. Individual cells, which were not in physical contact to any neighboring cell during the whole experiment, were identified. The locomotion of each cell was calculated by measuring the position of its nucleus at the beginning and end of the 8-h recording period. Results of three independent experiments (6–7 cells) are expressed as mean ± SEM. Cell locomotion of different clones was compared using an independent Student's *t* test.

Fibrin Gel Assay

Fibrin gels were prepared as previously described (Montesano *et al.*, 1990). Cells were seeded in suspension into 500-μl fibrin gels at 1 $\times$ 10^4 cells per gel. Five hundred microliters of complete culture medium was added to each well above the fibrin gels. All experiments were performed in the absence or presence of 200 kIU/ml trasylol, which was added to both gel and medium at the time of seeding. Medium (±trasylol) was renewed every 2–3 days. Between 4 and 9 days after seeding, cultures were used for dye injections or were fixed in situ overnight in 2.5% glutaraldehyde in 0.1 M cacodylate buffer (pH 7.4) and photographed using an inverted phase contrast microscope (Nikon). The surface area of individual cysts was determined from photographs and expressed as mean ± SEM. Surface area of different clones was compared using an independent Student's *t* test.

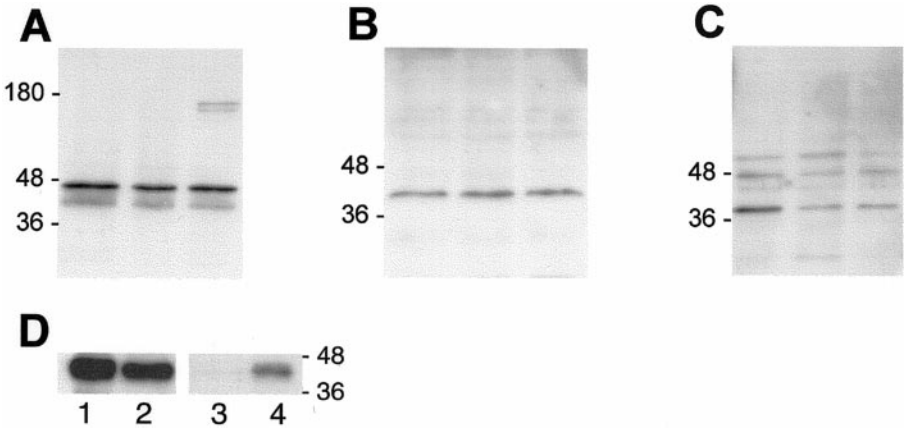

Figure 2. Western blot analysis of Cx43, Cx40, and Cx37 expression. (A–C) Aliquots of protein extracts collected from parental bEnd.3 cells (left lanes), bEnd.3/3243H7 cells (middle lanes), and bEnd.3/Cx43βGal cells (right lanes) were subjected to SDS/PAGE in 12% polyacrylamide gels. After transfer to nitrocellulose membranes, the blots were probed using Cx43 (A), Cx40 (B), or Cx37 (C) antibodies, with detection performed by chemiluminescence. (A) Anti-Cx43 antibody revealed several bands at 41–47 kDa, corresponding to the endogenous Cx43 protein and/or the chimeric 3243H7 protein, as well as two higher molecular weight bands at ~160 kDa, corresponding to the Cx43βGal fusion protein. (B) Anti-Cx40 antibody revealed a band at 42 kDa, corresponding to the Cx40 protein. (C) Anti-Cx37 antibody revealed a band at 39 kDa, corresponding to the Cx37 protein, as well as two nonspecific bands at ~48–60 kDa, which were also observed after incubation with preimmune serum. (D) Protein extracts of parental bEnd.3 cells (lanes 1 and 3) and bEnd.3/3243H7 cells (lanes 2 and 4) were immunoprecipitated with anti-HA antibodies. Supernatants (lanes 1 and 2) and immunoprecipitates (lanes 3 and 4) were collected, blotted, and probed with anti-Cx43 antibodies. Native Cx43 was slightly less abundant in bEnd.3/3243H7 cells (lane 2) than in parental cells (lane 1). The precipitated chimeric connexin could be specifically recognized in bEnd.3/3243H7 cells (lane 4).

Zymography and Reverse Zymography

Confluent monolayers of cells in 35-mm culture dishes were washed twice with serum-free DME, and 1.5 ml serum-free DME containing 200 kIU/ml trasylol was added. Sixteen hours later, cell extracts and culture supernatants were prepared and analyzed by zymography and reverse zymography as previously described (Vassali *et al.*, 1984; Montesano *et al.*, 1990). Cell numbers were determined in a second set of dishes processed in parallel, and cell extract and culture supernatant samples were analyzed on the basis of cell equivalents.

RESULTS

Expression of Dominant Negative Connexin Inhibitors

To analyze the effects of dominant negative connexin inhibitors on endothelial wound repair, we isolated stable transfectant clones. Among the 12 clones obtained, 2 transfected with p3243H7Et (B3 and B5) and 2 transfected with pEFZ (D1 and D2) were selected for further screening. First, we performed dye coupling experiments on subconfluent cultures of each clone, in order to examine the effects of 3243H7 or Cx43-βGal on cell coupling (Table 1). In average, microinjection of Lucifer Yellow into parental bEnd.3 cells resulted in the labeling of ~9 cells. Transfection with the hygromycin resistance gene alone (clone A3) did not affect the extent of dye diffusion. In contrast, clones B3, B5, D1, and D2 showed a significant ($p < 0.01$) reduction in the extent of Lucifer Yellow diffusion that was limited on average to 2–4 cells. Second, we performed RT-PCR to confirm the expression of the dominant negative inhibitors. mRNA was extracted from the different bEnd.3 cell clones and reverse transcribed into cDNA. The cDNA was PCR-amplified using primers recognizing Cx43, 3243H7, or Cx43-βGal and analyzed by gel electrophoresis. As shown in Figure 1A, a cDNA fragment of 334 bp, corresponding to the expected size for Cx43, was detected in parental bEnd.3 cells and all transfectant clones (lanes 1–5). cDNA fragments of the expected size for 3243H7 (421 bp, Figure 1A, lanes 7 and 8) and for Cx43-βGal (383 bp; Figure 1A, lanes 10 and 11) were detected in clones B3 and B5 and clones D1 and D2, respectively. Control PCRs on parental bEnd.3 cells with primers recognizing 3243H7 or Cx43-βGal did not result in an amplification product (Figure 1A, lanes 6 and 9, respectively), neither did a PCR without reverse transcriptase, indicating that our mRNA samples were free of genomic DNA. As can be seen in Table 1, clones B5 (= hereafter referred to as bEnd.3/3243H7 cells) and D2 (= hereafter referred to as bEnd.3/Cx43-βGal cells) displayed the largest inhibition of cell-to-cell coupling and, for this reason, were selected for further experiments.

The subcellular localization of 3243H7 and Cx43-βGal was next examined by immunofluorescence. After incubation with anti-HA antibodies, bEnd.3/3243H7 cells showed a strong perinuclear labeling and a diffuse fluorescence throughout the cytoplasm. No labeling, however, could be observed at the sites of contact between these cells (Figure 1B). A similar labeling pattern could be observed in bEnd.3/3243H7 cells using Cx43 antibodies (Figure 1C). In contrast, bEnd.3/Cx43-βGal cells incubated with anti-βGalactosidase or anti-Cx43 antibodies exhibited a punctate labeling at apposed plasma membranes, together with a strong perinuclear signal (Figure 1, D and E). Control experiments using anti-HA or anti-βGalactosidase antibodies on parental bEnd.3 cells or using secondary antibodies alone yielded no significant labeling.

Relative connexin levels in parental bEnd.3 cells were compared with those in bEnd.3/3243H7 and bEnd.3/Cx43-βGal cells by Western blot analysis. Total protein preparations were isolated from subconfluent monolayers of each clone, and equal amounts of protein were blotted and probed with anti-Cx43, anti-Cx40, or anti-Cx37 antibodies. Cx43 antibodies recognized a triplet of proteins migrating between 41 and 47 kDa in all extracts (Figure 2A). No difference in the intensity of this triplet was observed between parental cells, bEnd.3/3243H7 cells, and bEnd.3/

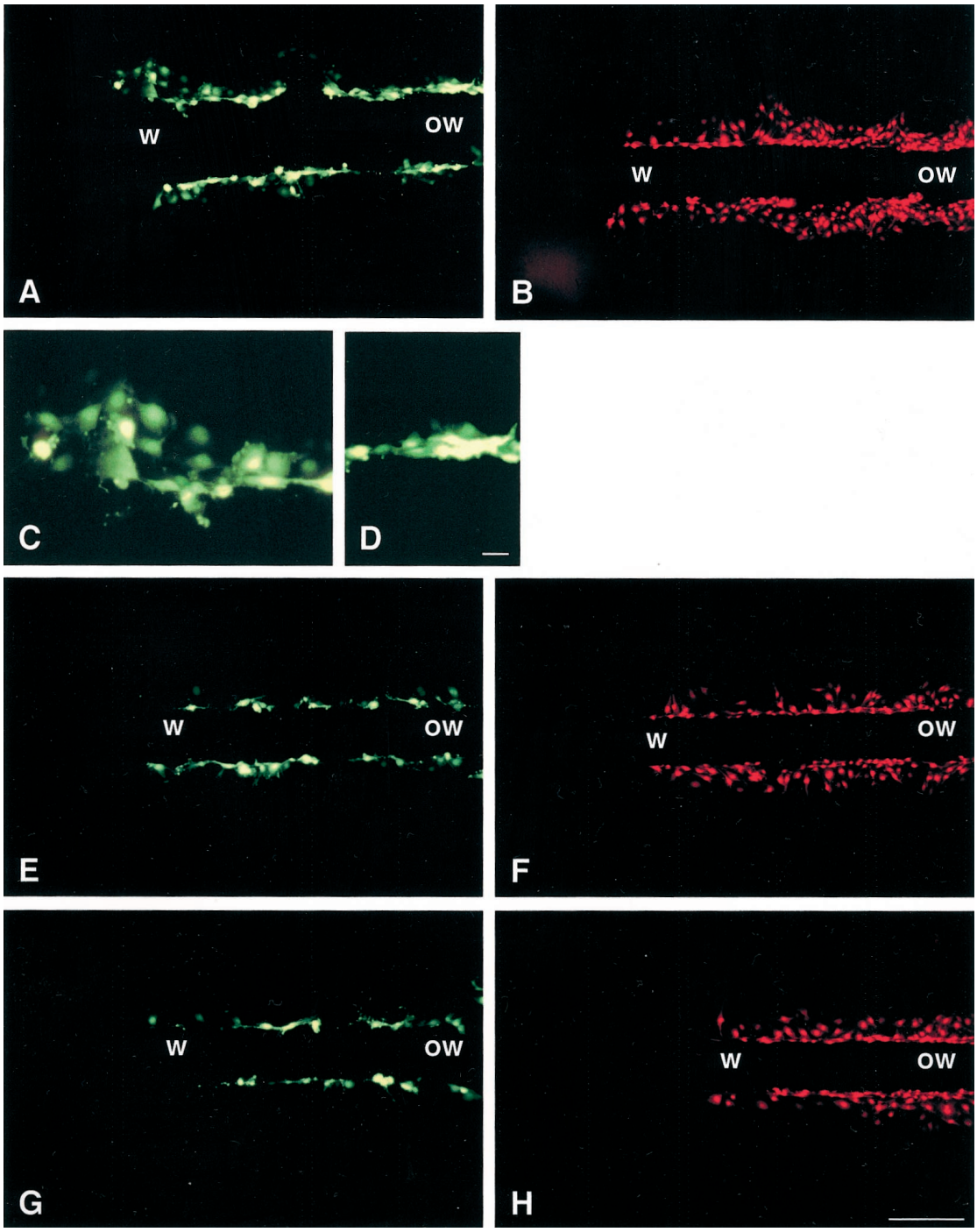

Figure 3. Junctional communication of parental and transfected bEnd.3 cells 24 h after wounding, as determined by scrape loading. (A–H) Fluorescence views showing the wound (w) and outside the wound (ow) regions of monolayers after loading with Lucifer Yellow (A, E, and G) or propidium iodide (B, F, and H) along a scrape perpendicular to the original wound. (A) In the wound region (w), Lucifer Yellow has labeled several rows of parental bEnd.3 cells on either side of the scrape line, whereas outside of the wound (ow), the fluorescent tracer labeled only one or two rows of cells. (B) Under these conditions, propidium iodide appeared less extensively exchanged between cells at the wound (w) than in the outside the wound (ow) region. (C and D) High-magnification views of the wound and outside the wound regions shown in A. (E–H) After transfection with cDNAs coding for 3243H7 (E and F) or Cx43βGal (G and H), the diffusion of both Lucifer Yellow and propidium iodide was reduced compared with that observed in parental cells. In addition, the increase in Lucifer Yellow diffusion that can be observed in the wound region of parental cells was no longer seen in bEnd.3/3243H7 (E) and bEnd.3/Cx43βGal cells (G). The decrease in propidium iodide diffusion that can be observed in the wound region of parental cells, however, can still be observed in either of the transfected clones (F and H). Bar: A, B, and D–G, 130 μm; C and D, 20 μm.

Table 2. Cell-to-cell coupling of parental and transfected bEnd.3 cells 24 h after wounding, as determined by microinjection of Lucifer Yellow

Clone	Location	Cell-to-cell coupling	SEM	Number of injections
bEnd.3	W	12.3[a]	0.5	10
bEnd.3	Ow	5	0.3	10
B5	W	3.1[b]	0.3	10
B5	Ow	1.7	0.3	10
D2	W	3.5[b]	0.3	10
D2	Ow	1.6	0.2	10

The number of cells labeled with Lucifer Yellow after a 3-min microinjection was counted 24 h after wounding in both wound (W) and 'outside of the wound' (Ow) regions of the parenteral bEnd.3 cell line, a clone of bEnd.3 cells transfected with 3243H7 cDNA (B5), or Cx43βGal cDNA (D2). Parental bEnd.3 cells of the confluent outside of the wound regions were coupled on average to ~5 neighboring cells. This extent of coupling was significantly ([a] $p < 0.01$) increased to ~12–13 neighboring cells at the wound. Both bEnd.3/3243H7 and bEnd.3/Cx43βGal cells showed reduced coupling, being usually coupled to only one neighboring cell in the outside the wound region. The extent of Lucifer Yellow transfer in the wound region marginally increased between cells expressing the dominant negative connexins and, in all cases, was significantly ([b] $p < 0.01$) decreased compared with parental cells.

Cx43-βGal cells in three replicate experiments. In addition, a doublet of proteins with an apparent molecular weight of ~160 kDa was recognized by Cx43 antibodies only in bEnd.3/Cx43-βGal cells. The latter doublet was also recognized by βGalactosidase antibodies, and is thus likely to represent the fusion protein. The electrophoretic mobility of 3243H7 is expected to be between 41 and 47 kDa, making it difficult to distinguish the chimeric protein from native Cx43 in Western blots. Therefore, we performed immunoprecipitation experiments with anti-HA antibodies on lysates of parental and bEnd.3/3243H7 cells. The supernatants and immunoprecipitated proteins were blotted and probed with anti-Cx43 antibodies. The Cx43 band detected in the supernatant of parental bEnd.3 cells was more prominent than the one of bEnd.3/3243H7 cells (Figure 2D, lanes 1 and 2). In addition, the immunoprecipitated chimeric protein could be recognized with anti-Cx43 antibodies in bEnd.3/3243H7 cells and not in parental cells (Figure 2D, lanes 3 and 4). Cx40 antibodies recognized a single band at ~42 kDa in protein extracts from all clones (Figure 2B). This Cx40 band was of equal intensity in parental bEnd.3 cells, bEnd.3/3243H7 cells, and bEnd.3/Cx43-βGal cells. Cx37 antibodies recognized a band at ~39 kDa in protein extracts from parental bEnd.3 cells (Figure 2C). This Cx37 band was more prominent in parental bEnd.3 cells than in bEnd.3/3243H7 and bEnd.3/Cx43-βGal cells. In addition, two bands of unknown identity at ~48 and 60 kDa were observed in all extracts. These bands, however, could also be observed after incubation with preimmune serum and, thus, were considered nonspecific. Western blotting on total protein extracted from HeLa cells transfected with Cx43, Cx40, or Cx37 was performed as a positive control. With each antibody used, a similar band pattern was obtained with extracts of bEnd.3 and transfected HeLa cells (see Figure 5, C, F, and I, lanes 1).

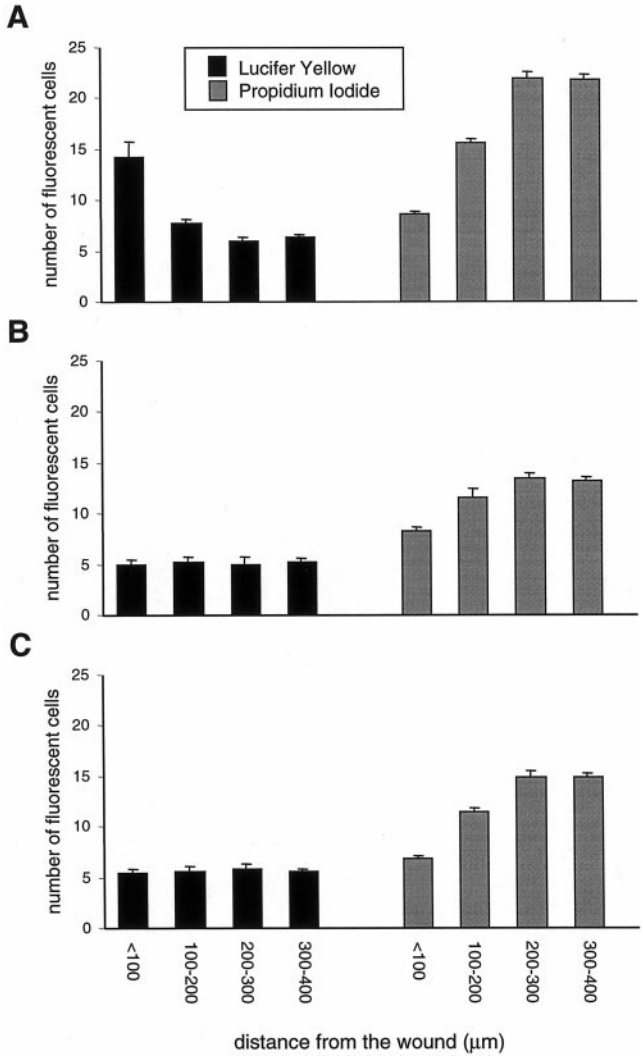

Figure 4. Quantification of junctional communication of parental and transfected bEnd.3 cells 24 h after wounding, as determined by scrape loading. The number of cells labeled with Lucifer Yellow or propidium iodide was counted along the scrape and expressed per bands of 100-μm thickness, starting from the wound edge toward the confluent region of the culture in parental bEnd.3 cells (A), bEnd.3/3243H7 cells (B), and bEnd.3/Cx43βGal cells (C). (A) Transfer of Lucifer Yellow is significantly ($p < 0.01$) increased and that of propidium iodide significantly ($p < 0.01$) decreased at the wound edge, compared with outside of the wound regions between parental bEnd.3 cells. (B and C) In bEnd.3/3243H7 and bEnd.3/Cx43βGal cells, Lucifer yellow diffusion is similar at the wound edge and in outside the wound regions. In contrast, propidium iodide diffusion significantly ($p < 0.01$) decreased at the wound edge compared with outside of the wound regions in both transfectants. Values are mean ± SEM of five experiments.

Cell-Cell Communication after Wounding

To assess whether migrating bEnd.3 cells displayed altered cell-to-cell communication, confluent monolayers were wounded and dye diffusion was examined after 24 h within the first 8 cell rows (~100 μm) from the wound edge and at

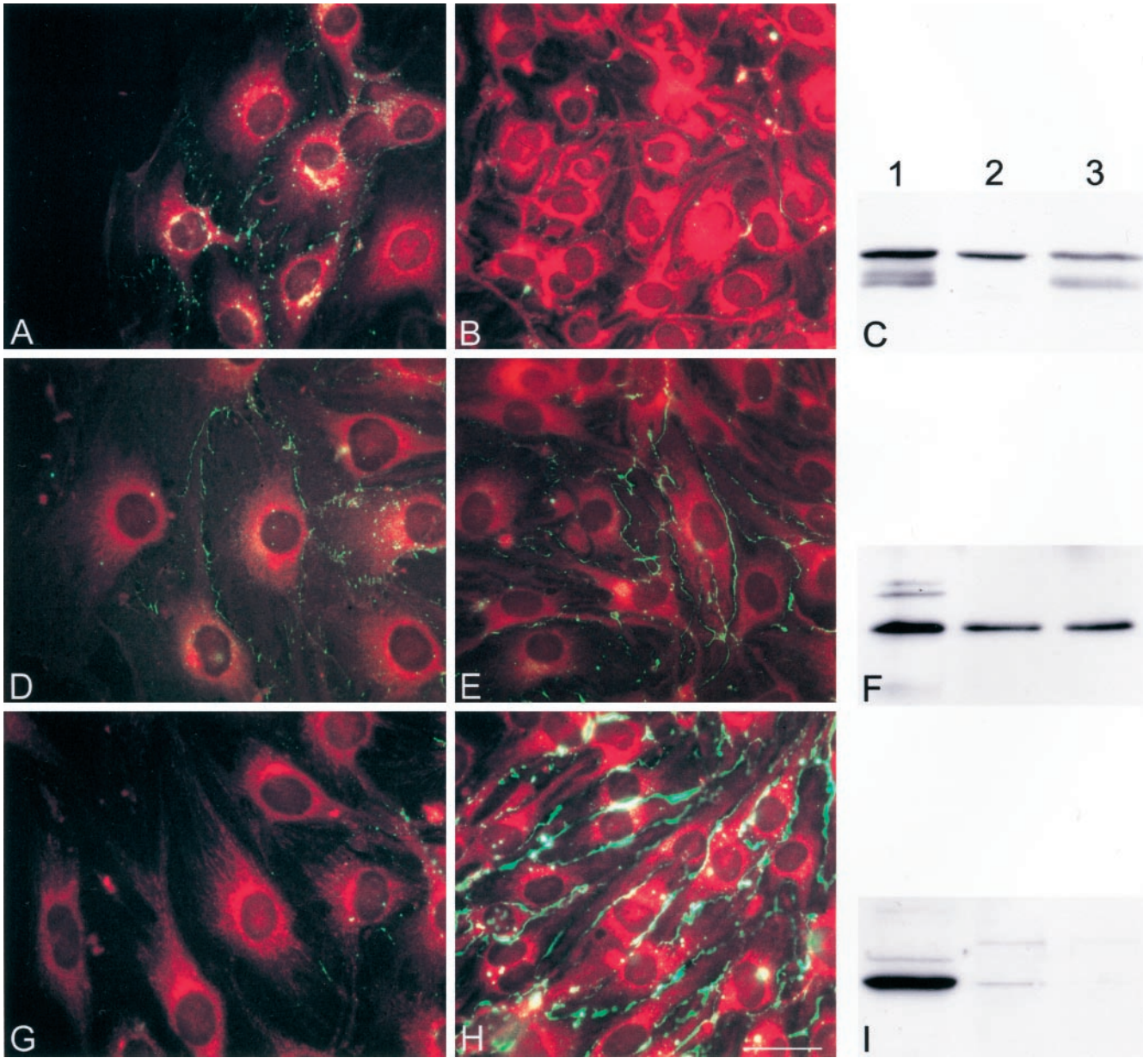

Figure 5. Cx43 is up-regulated and Cx37 down-regulated at the wound edge in parental bEnd.3 cells, 24 h after wounding. (A, B, D, E, G, and H) Representative fluorescence micrographs of the wound (A, D, and G) and outside the wound regions (B, E, and H) of parental bEnd.3 cells after immunostaining with anti-Cx43 (A and B), anti-Cx40 (D and E), or anti-Cx37 (G and H) antibodies. Cells are counterstained with Evans Blue. (A) Punctate Cx43 immunoreactivity (green labeling) was induced along the lateral borders of adjacent cells in the wound area. (B) This immunoreactivity was virtually absent at cell-to-cell contacts in outside the wound regions. (D and E) Cx40 immunoreactivity can be detected in regions of cell-to-cell contact in both wound and outside of the wound regions. (G) Cx37 immunoreactivity was not detected in the first rows of cells lining the wound. (H) In contrast, this immunoreactivity is abundantly detected in areas outside the wound. Bar, 30 μm. (C, F, and I) Western blots of proteins extracted from HeLa transfectants (lanes 1), confluent (lanes 2), or multiple wounded cultures of bEnd.3 cells (lanes 3) probed with Cx43 (C), Cx40 (F), or Cx37 (I) antibodies. (C) Anti-Cx43 antibody revealed several bands at 41–47 kDa in control HeLaCx43 cells. A similar band pattern was detected in bEnd.3 cells from multiple wounded cultures. In confluent bEnd.3 cell cultures only a single band a 47 kDa was detected. (F) Anti-Cx40 antibody revealed a major band at 42 kDa in control HeLaCx40 cells. Cx40 bands of equal intensity were detected in multiple wounded and confluent bEnd.3 cell cultures. (I) Anti-Cx37 antibody revealed a major band at 39 kDa in control HeLaCx37 cells. This band could be readily detected in confluent bEnd.3 cell cultures, whereas it was virtually absent in multiple wounded cultures.

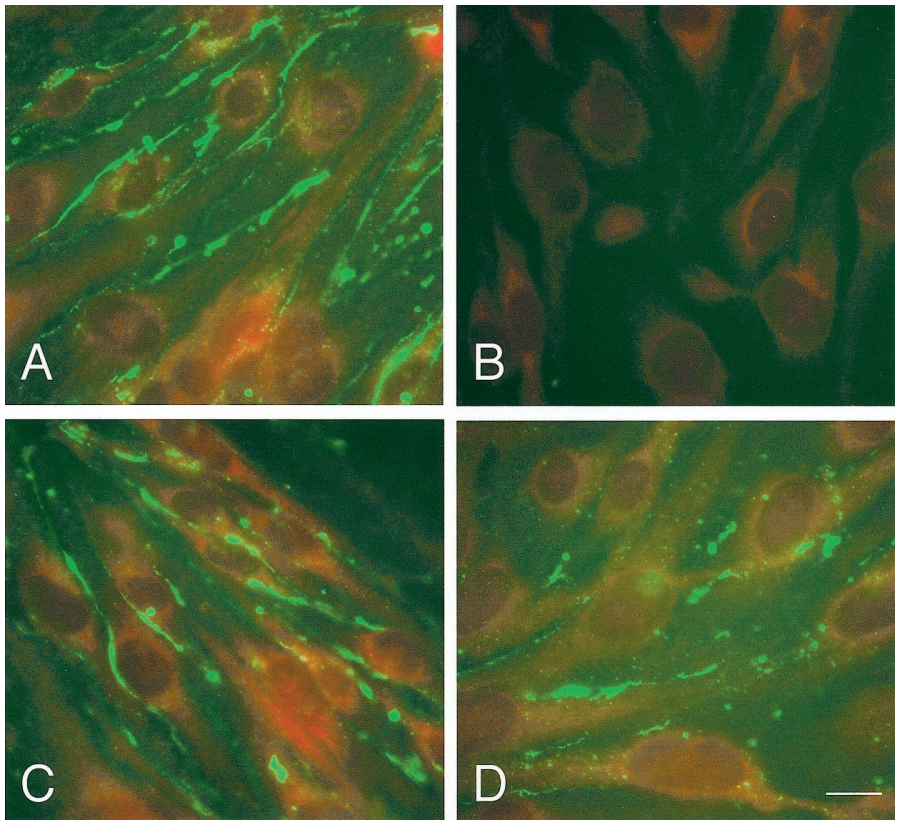

Figure 6. The abundant Cx37 immunostaining of bEnd.3 cells is reproduced with different specific antibodies. (A–D) Representative fluorescence micrographs of outside the wound regions of parental bEnd.3 cells after immunostaining with several anti-Cx37 antibodies directed against different epitopes, that is, amino acids 315–331 (A), 229–333 (C), and 266–281 (D), or with preimmune serum (B). Cells are counterstained with Evans Blue. A similarly abundant immunoreactivity was observed with all the three antibodies to Cx37 that were tested but not with a preimmune serum. Bar, 10 μm.

a distance from the wound. Using scrape loading (Figures 3, A and C and 4A) and microinjection (Table 2), extensive diffusion of Lucifer Yellow was observed between parental cells situated at the wound edge. In contrast, a much lower extent of Lucifer Yellow diffusion was observed between cells situated outside of the wound in the same monolayers (Figures 3, A and D, and 4A). Opposite observations were made using propidium iodide. The intercellular diffusion of this dye was decreased at the wound edge compared with that observed between cells situated outside of the wound (Figures 3B and 4A).

Expression of the dominant negative connexins 3243H7 or Cx43-βGal reduced the extent of intercellular diffusion of both Lucifer Yellow and propidium iodide (Figures 3 and 4). Moreover, the increase in Lucifer Yellow transfer observed in the wound region of parental bEnd.3 cells was severely mitigated in both bEnd.3/3243H7 and bEnd.3/Cx43-βGal cells (Figures 3, A, C, E, and G, and 4). However, the decrease in propidium iodide diffusion observed in the wound region of parental bEnd.3 cells was still maintained in cells expressing 3243H7 or Cx43-βGal (Figures 3, B, D, F, and H, and 4).

Cx Expression after Wounding

We next examined whether the changes in cell-to-cell coupling at the wound edge of parental bEnd.3 cells were related to changes in connexin expression using immunocytochemistry and Western blotting. Twenty-four hours after wounding, a punctate Cx43 immunolabeling was observed along the membranes of contacting bEnd.3 cells in the wound region (Figure 5A). However, at that time much less Cx43 labeling was detected outside the wound (Figure 5B). This difference was confirmed in Western blots of total protein isolated from confluent and multiple-wounded monolayers (Figure 5C). Indeed, Cx43 antibodies recognized a triplet of proteins migrating between 41 and 47 kDa in bEnd.3 cell extracts from wounded cultures (lane 3), whereas only a single band at 47 kDa was found in extracts of the same cells derived from confluent nonwounded cultures (lane 2). As illustrated in Figures 5, D and E, Cx40 immunostaining was similarly distributed along apposed plasma membranes in both wounded and nonwounded areas. This was confirmed in Western blots where Cx40 antibodies recognized a single band of equal intensity in bEnd.3 cell extracts from both confluent and wounded cultures (Figure 5F, lanes 2 and 3). Immunostaining with anti-Cx37 antibodies revealed almost no signal at the wound edge, whereas intense labeling was present along the membranes of bEnd.3 cells outside the wound (Figure 5, G and H). This unusual, almost continuous labeling was considered specific, inasmuch as it was observed using different antibodies to three distinct epitopes of Cx37 (Figure 6, A, C, and D, respectively) was abolished in the presence of only the secondary antibodies or preimmune serum (Figure 6B), and differed from that observed with antibodies to Cx43 (Figure 5B) or to the tight junction-associated protein ZO-1. However, this labeling did not correlate with an obvious increase in gap junction plaques, as assessed by freeze-fracture elec-

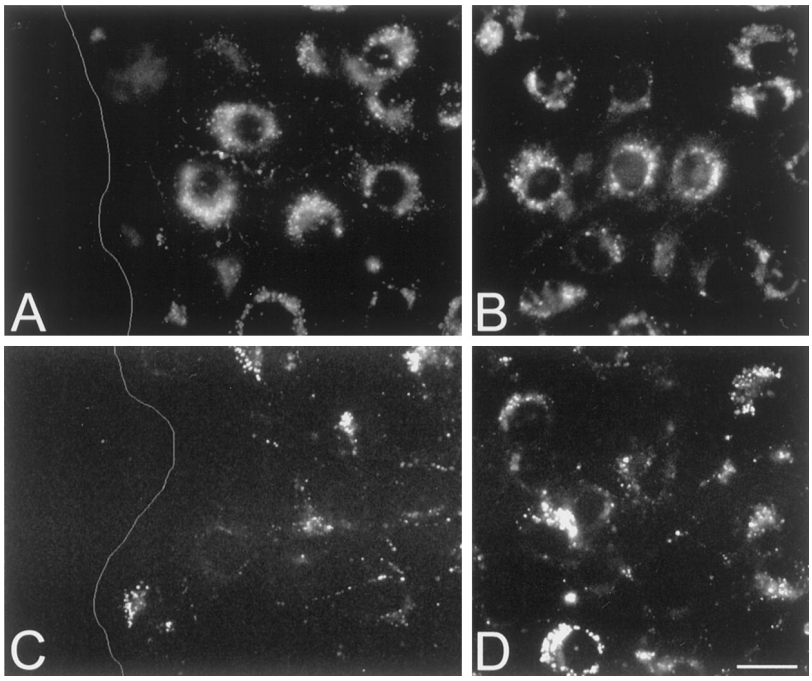

Figure 7. Inhibition of wound-induced Cx43 up-regulation in bEnd.3 cells expressing dominant negative connexins. (A–D) Representative fluorescence micrographs of the wound (A and C) and outside the wound region (B and D) of bEnd.3/3243H7 cells (A and B) and bEnd.3/Cx43βGal cells (C and D), 24 h after wounding. Cx43 immunoreactivity was detected predominantly in the perinuclear region. No obvious increase in Cx43 labeling was observed in the wound region of either transfected clone. Bar, 22 μm. White line (A and C) represents the wound edge.

tron microscopy. As illustrated in Figure 5I, Cx37 antibodies clearly recognized a band of ~39 kDa in protein extracts from Cx37-transfected HeLa cells, which were used as a positive control (lane 1). A band of similar electrophoretic mobility was observed in extracts from confluent monolayers of bEnd.3 cells (Figure 5I, lane 2) but was barely detectable in extracts from wounded cultures (Figure 5I, lane 3). Thus, upon wounding of parental bEnd.3 cells, the expression of Cx43 was up-regulated, that of Cx37 was down-regulated, and that of Cx40 was unaffected at the wound edge.

In order to assess whether expression of dominant negative connexins affected the wound-induced changes in the expression of native connexins, immunofluorescence labeling was performed on cultures of transfected bEnd.3 cells, 24 h after wounding. As shown in Figure 7, staining with anti-Cx43 antibodies revealed a strong perinuclear labeling and almost no labeling at cell-to-cell contacts of both bEnd.3/3243H7 and bEnd.3/Cx43-βGal cells (Figures 7, A and B, and 7, C and D, respectively). Moreover, the up-regulation of Cx43 expression, seen at the wound edge of parental bEnd.3 cells, was severely mitigated in cells expressing the dominant negative inhibitors (cf. Figure 5A with Figures 7A and 7C). Cx37 expression levels were lower in bEnd.3/3243H7 and bEnd.3/Cx43-βGal cells, compared with parental cells (cf. Figures 8, B and D, with Figure 5C). However, immunolabeling of wounded cultures revealed that the down-regulation of Cx37 expression at the wound edge was not prevented by either dominant negative inhibitor (Figure 8, A and C).

Wound Repair

To determine the effects of dominant negative Cx inhibitors on the kinetic of endothelial wound repair, confluent monolayers were mechanically wounded and the distance between the two wound edges was monitored as a function of time. As can be seen in Figure 9, in parental bEnd.3 cells complete closure of the 6-mm wound was reached after 8.2 $\pm$ 0.4 days (mean $\pm$ SEM; n = 5 monolayers). Cells expressing dominant negative connexins, on the other hand, required significantly more time: complete closure of the 6-mm wound was reached after 13 $\pm$ 0.5 days and 11 $\pm$ 0.4 days by bEnd.3/3243H7 (n = 5) and bEnd.3/Cx43-βGal cells (n = 5), respectively. In contrast, we observed that proliferation rates of parental bEnd.3 cells, bEnd.3/3243H7 cells, and bEnd.3/Cx43-βGal cells were not different at the wound edge and at distance of the wound, as evaluated by cumulative cell numbers (Figure 10A) and BrdU incorporation (Figure 10B). Furthermore, individual bEnd.3 were found to migrate over a distance of 249 $\pm$ 48 μm in 8 h (n = 7 cells), as determined with time-lapse video imaging. This rate of cell locomotion was not different in single bEnd.3/3243H7 and bEnd.3/Cx43-βGal cells (247 $\pm$ 48 μm/8 h (n = 6) and 237 $\pm$ 42 μm/8 h (n = 6), respectively).

In order to test whether transfection of dominant negative Cx inhibitors affected other cell functions, parental and transfected bEnd.3 cells were grown within fibrin gels and the proteolytic activity of urokinase-type plasminogen activator (uPA) and plasminogen activator inhibitor (PAI-1) was determined. As expected, parental bEnd.3 cells proliferated rapidly and formed large cyst-like structures in the fibrin gels (Figure 11A). This process of cyst formation was not altered in either bEnd.3/3243H7 or bEnd.3/Cx43-βGal cells, as evaluated by comparing cyst surface areas after 2 or 4 days of culturing (Figure 11, C, E, and G). In contrast, the differences in diffusion of Lucifer Yellow, observed in monolayers of parental and transfected bEnd.3 cells, were also observed in cysts grown of these cells. Indeed, microinjec-

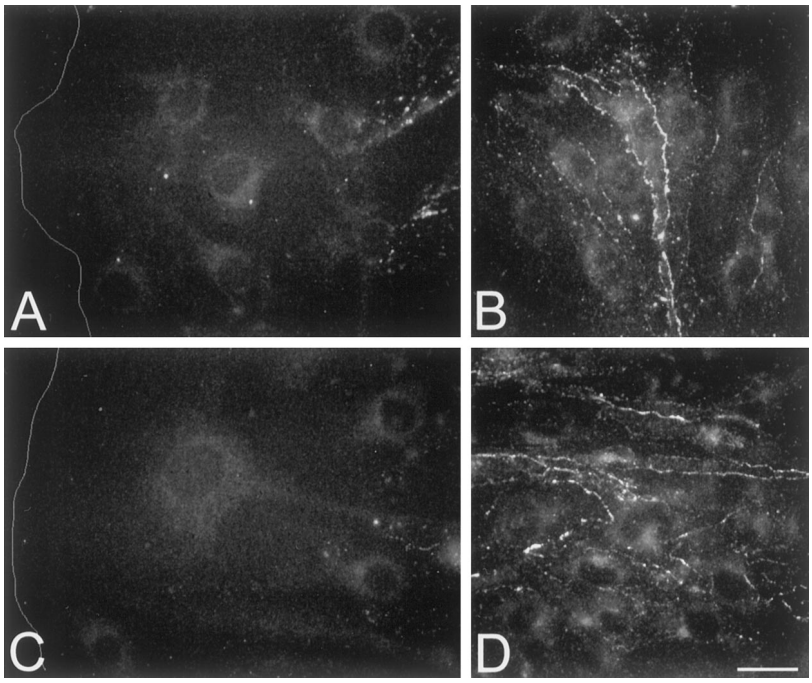

Figure 8. Wound-induced down-regulation of Cx37 is not prevented in bEnd.3 cells expressing dominant negative connexins. (A–D) Representative fluorescence micrographs of the wound (A and C) and outside the wound region (B and D) of bEnd.3/3243H7 cells (A and B) and bEnd.3/Cx43βGal cells (C, D) 24 h after wounding. In both transfected clones, Cx37 immunoreactivity is abundantly detected in areas outside the wound but absent in the first rows of cells lining the wound edge. Bar, 22 μm. White line (A and C) represents the wound edge.

tion of Lucifer Yellow into cysts grown from parental cells resulted in the labeling of 8 cells, whereas the dye labeled an average of ~2 cells in cysts of bEnd.3/3243H7 and bEnd.3/Cx43-βGal cells (Table 1). When parental or transfected bEnd.3 cells were grown in fibrin gels in the presence of Trasylol, a broad spectrum serine protease inhibitor, cyst formation was inhibited (Figure 11, B, D, and F). Zymographic and reverse zymographic analysis revealed high levels of activity of uPA and detectable levels of activity of PAI-1 in all clones. No clear differences in the activity of uPA and PAI-1 were detected in cell extracts and culture supernatants of parental and transfected cells (not shown).

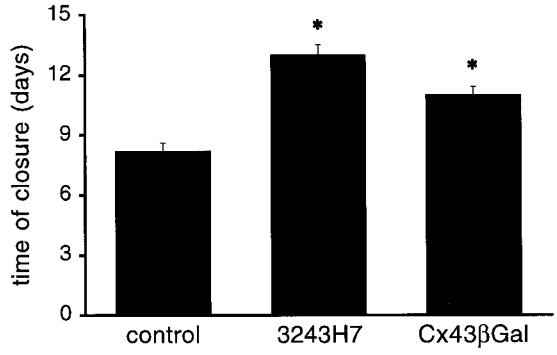

Figure 9. Wound repair of parental and transfected bEnd.3 cells. Confluent monolayers were mechanically wounded with a 6-mm-wide rubber policeman in five independent cultures of parental, bEnd.3/3243H7, or bEnd.3/Cx43βGal cells. Cultures were observed every day until complete closure of the wound was reached. Values are mean ± SEM. Time for complete wound repair in bEnd.3/3243H7 and bEnd.3/Cx43βGal cell cultures was significantly (*$p < 0.01$) increased over that in parental cell cultures.

DISCUSSION

Previous studies have documented a possible role for gap junction-mediated communication in endothelial wound repair (Larson and Haudenschild, 1988; Pepper *et al.*, 1989, 1992). The recent availability of dominant negative connexin inhibitors made it possible to specifically perturb gap junction formation and to directly investigate the influence of gap junctional communication on endothelial cell function. We show here that abnormal patterns of intercellular communication alter wound repair without affecting other endothelial cell properties.

Migrating endothelial cells have been reported to display increased, unaltered, or even decreased levels of intercellular communication upon wounding (Larson and Haudenschild, 1988; Pepper *et al.*, 1989, 1992; Gabriels and Paul, 1993). The cause of this differential response on endothelial wounding is still unknown, although it has been suggested that cell origin might play a role (Pepper *et al.*, 1992). Indeed, endothelial cells differ markedly along the vascular tree with respect to their surface phenotype and protein expression (Cines *et al.*, 1998). In addition, the presence and amount of different connexins in cultured endothelial cells may determine their reaction to wounding. At variance with many other cultured endothelial cell types, the bEnd.3 cells we used express in combination the three connexins (Cx43, Cx40, and Cx37), which are expressed by endothelial cells in vivo. Moreover, the relative expression levels of these connexins were maintained for over 40 passages in culture. The bEnd.3 cell line originates from primary mouse brain endothelial cells that were transduced with a PymT-expressing retrovirus (Montesano *et al.*, 1990). PymT-transformed endothelial cells retain important characteristics of differentiated endothelium, such as expression of the endothelial proteins vWF, CD31, MECA-32, and the VEGF receptor 2, internal-

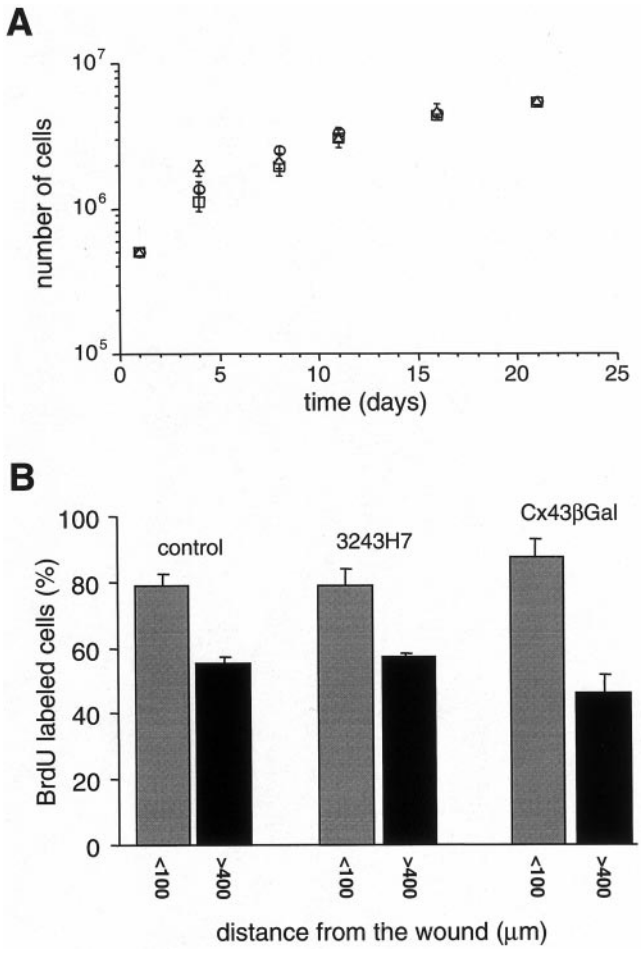

Figure 10. Proliferation rates of parental and transfected bEnd.3 cells. (A) Cells were seeded at 5×10^5 per 25-cm^2 culture flask, trypsinized, and counted every 3–4 days. Cumulative cell numbers are represented over 21 days in culture. Values are mean ± SEM. □, parental bEnd.3 cells; ○, bEnd.3/3243H7 cells; and △, bEnd.3/Cx43βGal cells. (B) BrdU incorporation was examined by fluorescence, and total cell number was determined after counterstaining of the cells with Evans Blue. The percentage of BrdU-labeled cells was determined in a band of 100-μm thickness along the edge of the endothelial wound (gray bars) and at >400 μm distance from it in the confluent part of the culture (black bars). BrdU incorporation in parental cells and transfectants are not significantly ($p < 0.05$) different from each other in either wound or outside the wound areas. n = 5 experiments.

ization of acetylated LDL, and induction of cytokines and cellular adhesion molecules upon stimulation with IL-1 or TNF-α (Pepper *et al.*, 1997). Thus, bEnd.3 cells may serve as a well-defined model for studies aimed at elucidating the role of gap junctions in endothelial cell function.

Wound-induced migration of bEnd.3 cells was associated with an increase in Cx43 expression, an effect that has also been reported for capillary endothelial cells (Pepper *et al.*, 1989). Under these conditions, we observed that migrating bEnd.3 cells also display decreased levels of Cx37 expression, whereas Cx40 expression levels were unaltered. The expression level of another junction-associated protein, ZO-1, was also not detectably affected 24 h after wounding. The differential change in the expression of specific connexin types was associated with a marked change in the pattern of intercellular communication. Indeed, the use of two fluorescent dyes, which feature differential permeabilities through Cx43 and Cx37 gap junction channels (Elfgang *et al.*, 1995), revealed increased cell-to-cell diffusion of Lucifer Yellow but decreased propidium iodide diffusion at the wound edge. These observations demonstrate, a connexin-specific modulation of intercellular communication between migrating cells, presumably to favor wound repair.

The recent generation of the chimeric protein 3243H7 and the fusion protein Cx43-βGal, which both act as dominant negative inhibitors of gap junction formation (Paul *et al.*, 1995; Sullivan and Lo, 1995), provides tools to directly study the involvement of intercellular communication in cell migration. We have stably transfected bEnd.3 cells with cDNAs coding for each of these dominant negative connexins, as confirmed by RT-PCR and immunofluorescence. The expression of 3243H7 or Cx43-βGal in bEnd.3 cells resulted in a marked decrease in the extent of both Lucifer Yellow and propidium iodide diffusion under basal, nonwounded conditions and in a failure to increase Lucifer Yellow diffusion upon wounding. However, the mechanism by which the two dominant negative inhibitors affect gap junctional communication was not determined in this study. In agreement with observations in the early *Xenopus* embryo (Paul *et al.*, 1995), 3243H7 showed a diffuse intracellular localization and was absent at cell-to-cell contacts, suggesting altered intracellular trafficking of the chimeric protein. Cx43-βGal, on the other hand, was abundantly detected at regions of cell-to-cell contact as well as in the perinuclear cytoplasm. Whatever the mechanism, both dominant negative inhibitors similarly decreased basal expression of Cx37, without affecting that of Cx40. Although the effects on basal expression of Cx43 were small (bEnd.3/3243H7 cells) or absent (bEnd.3/Cx43-βGal cells), the increase in Cx43 at contact areas between migrating cells was largely prevented by either dominant negative inhibitor. Although the precise mechanism remains to be determined, our studies show that expression of 3243H7 or Cx43-βGal perturbed the pattern of gap junctional communication between bEnd.3 cells under basal and wounded conditions.

Expression of dominant negative inhibitors also markedly changed the rate of wound repair. The time to completely close a 6-mm wound required ~8 days in parental bEnd.3 cells. In contrast, this time was increased by 32–59% in the communication-perturbed transfected bEnd.3 cells. Differences in proliferation rate or in locomotion of individual cells are unlikely to account for this prolonged repair period, because these properties were similar in parental and transfected cells. In addition, dominant negative inhibitor proteins or mRNAs did not affect the fibrinolytic activity of endothelial cells embedded in three-dimensional fibrin gels (Montesano *et al.*, 1990). Indeed, transfected bEnd.3 cells formed similar large cyst-like structures and displayed similar extracellular proteolytic activity than parental cells, although dye coupling within cysts was markedly decreased by the dominant negative inhibitors. Thus, our results indicate that a specific alteration in the pattern of intercellular communication inhibits endothelial wound repair. A similar biological effect, that is, delayed closure of the wound, was

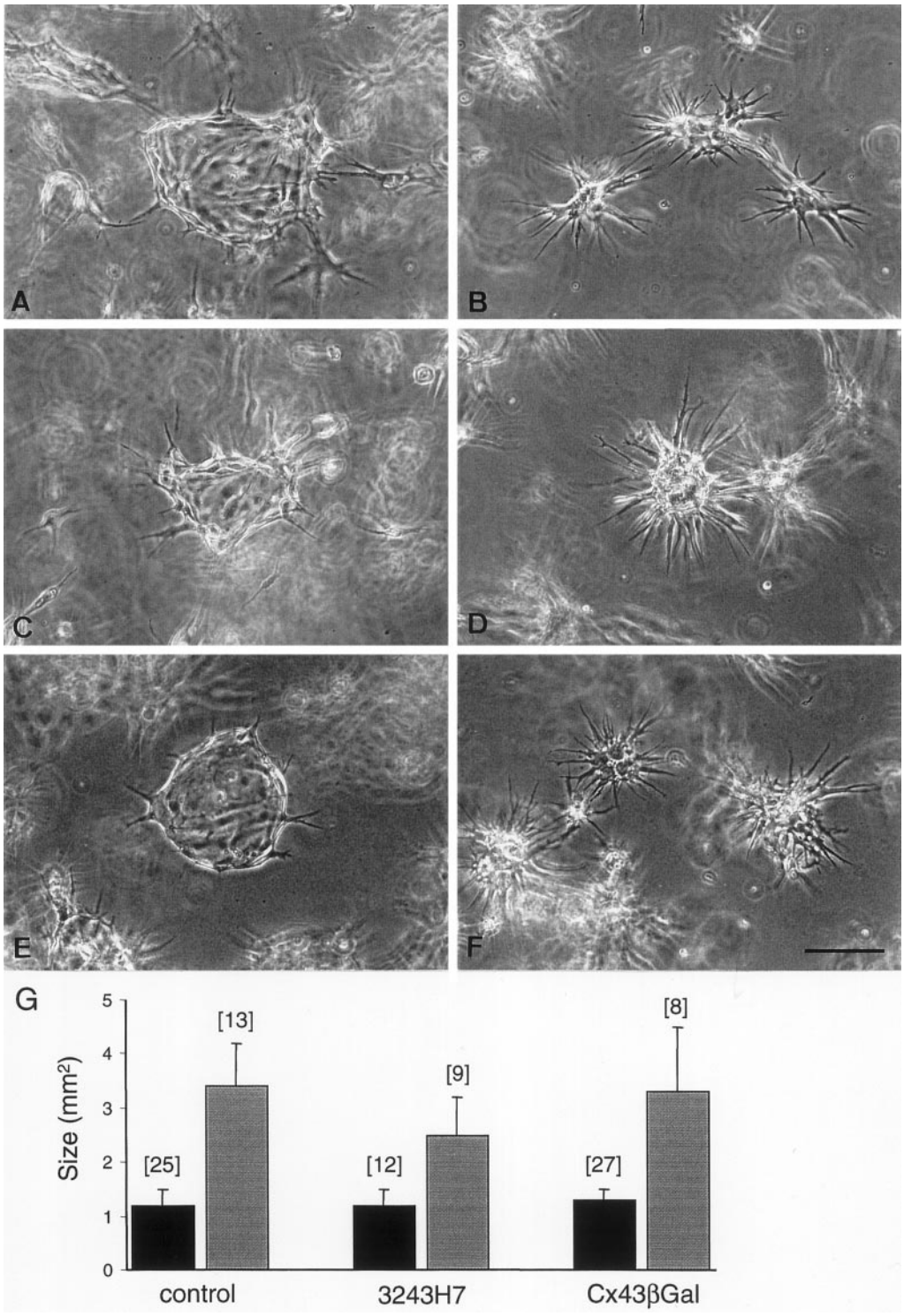

Figure 11. Morphogenetic behavior of parental and transfected bEnd.3 cells in three-dimensional fibrin gels. Cells were seeded into fibrin gels, grown in the absence (A, C, and E) or presence (B, D, and F) of Trasylol, and photographed by phase contrast microscopy after 2 days. (G) Parental bEnd.3 cells (A and B), bEnd.3/3243H7 (C and D), and bEnd.3/Cx43βGal (E and F) cells formed cysts whose formation could be inhibited by the serine protease inhibitor (B, D, and F). Bar, 120 μm. (G) The surface area of cysts formed of parental bEnd.3 cells, bEnd.3/3243H7, and bEnd.3/Cx43βGal cells was measured after 2 (black bars) and 4 (gray bars) days of culture. Average surface areas of different cells types are not significantly ($p < 0.05$) different from each other at either culture time. Numbers between in indicate the number of cysts measured.

observed after complete blockade of gap junctional communication by 5 μM 18-α-glycyrrhetinic acid. Whether the delay in wound repair is due to a loss in directionality of cell movement in migrating transfectants remains to be established.

In conclusion, we have shown that gap junctional communication serves to coordinate cell migration during endothelial repair. Although the link between gap junctional coupling and wound repair remains to be elucidated at a molecular level, the opposite change in Cx37 and Cx43 expression observed after wounding suggest that these two Cx types may differentially regulate the cell-to-cell transfer of factors important for the control of cell migration. During endothelial repair, stimulatory signals received by cells at the migration front may be passed via gap junction channels, presumably made of Cx43, to endothelial cells outside of the wound. Alternatively, the passage of inhibitory signals originating from endothelial cells in a confluent monolayer may not reach cells at the wound edge, presumably because of lack of Cx37 gap junction channels. In either case, the altered pattern of intercellular communication would help increasing the migration efficiency of a sheet of endothelial cells. Interestingly, the migration rate of neural crest cells is also affected by the level of gap junctional communication (Huang *et al.*, 1998), providing novel support to the hypothesis of a general role for gap junctions in the physiology of migratory cells (Pepper *et al.*, 1989, 1992). Altogether, our findings indicate that coordinated movement of a leading front of endothelial cells improves reendothelization of a denuded wound area and suggest that this may also be important for capillary sprouting during angiogenesis.

ACKNOWLEDGMENTS

We are grateful to Drs. D.L. Paul and C.W. Lo for providing antibodies and/or constructs containing dominant negative connexin inhibitors. We thank Dr. K. Willecke for providing us with HeLa transfectants, Dr. M. Chanson for critical reading of the manuscript and T. Dudez for helpful advice. We also thank A. Charollais, F. De Leon, C. Di Sanza, M. Quayzin, and E. Suter for technical assistance and Dr. J. Kiss and "the Epithelium Network" for use of their facilities. This work was supported by grants from the Swiss National Science Foundation (3100-053720 and 3100-043364.95), the E.E.C (QLG1-CT-1999-00516) and the "Fondation Carlos et Elsie Reuter" (265).

REFERENCES

Bastide, B., Neyses, L., Ganten, D., Paul, M., Willecke, K., and Traub, O. (1993). Gap junction protein connexin40 is preferentially expressed in vascular endothelium and conductive bundles of rat myocardium and is increased under hypertensive conditions. Circ. Res. *73*, 1138–1149.

Blackburn, J.P., Peters, N.S., Yeh, H.-I., Rothery, S., Green, C.R., and Severs, N.J. (1995). Upregulation of connexin43 gap junctions during early stages of human coronary atherosclerosis. Arterioscler. Thromb. Vasc. Biol. *15*, 1219–1228.

Blochlinger, K., and Dingelmann, H. (1984). Hygromycin B phosphotransferase as a selectable marker for DNA transfer experiments with higher eukaryotic cells. Mol. Cell. Biol. *4*, 2929–2931.

Bruzzone, R., Haefliger, J.-A., Gimlich, R.L., and Paul, D.L. (1993). Connexin40, a component of gap junctions in vascular endothelium, is restricted in its ability to interact with other connexins. Mol. Biol. Cell *4*, 7–20.

Bruzzone, R., White, T.W., and Paul, D.L. (1996). Connections with connexins: the molecular basis of direct intercellular signaling. Eur. J. Biochem. *238*, 1–27.

Cines, D.B., Pollak, E.S., Buck, C.A., Loscalzo, J., Zimmerman, G.A., McEver, R.P., Pober, J.S., Wick, T.M., Konkle, B.A., Schwartz, B.S., Barnathan, E.S., McCrae, K.R., Hug, B.A., Schmidt, A.M., and Stern, D.M. (1998). Endothelial cells in physiology and pathophysiology of vascular disorders. Blood *91*, 3527–3561.

Delorme, B., Dahl, E., Jarry-Guichard, T., Marics, I., Briand, J.P., Willecke, K., Gros, D., and Théveniau-Ruissy, M. (1997). Expression pattern of connexin gene products at early developmental stages of the mouse cardiovascular system. Circ. Res. *81*, 423–437.

Elfgang, C., Eckert, R., Lichtenberg-Fraté, H., Butterweck, A., Traub, O., Klein, R., Hülser, D., and Willecke, K. (1995). Specific permeability and selective formation of gap junction channels in connexin-transfected HeLa cells. J. Cell Biol. *129*, 805–817.

El-Fouly, M.H., Trosko, J.E., and Chang, C.-C. (1987). Scrape-loading and dye transfer. A rapid and simple technique to study gap junctional intercellular communication. Exp. Cell Res. *168*, 422–430.

Gabriels, J.E., and Paul, D.L. (1993). Characterization of connexin expression in rat aortic endothelial cells during in vitro wounding. Mol. Biol. Cell *4*, 329a.

Gabriels, J.E., and Paul, D.L. (1998). Connexin43 is highly localized to sites of disturbed flow in rat aortic endothelium but connexin37 and connexin40 are more uniformly distributed. Circ. Res. *83*, 636–643.

Goliger, J.A., and Paul, D.L. (1994). Expression of gap junction proteins Cx26, Cx31.1, Cx37, and Cx43 in developing and mature rat epidermis. Dev. Dyn. *200*, 1–13.

Gros, D., Jarry-Guichard, T., Ten Velde, I., De Mazière, A., Van Kempen, M.J.A., Davoust, J., Briand, J.P., Moorman, A.F.M., and Jongsma, H.J. (1994). Restricted distribution of connexin40, a gap junction protein, in mammalian heart. Circ. Res. *74*, 839–851.

Haefliger, J.A., Polikar, R., Schnyder, G., Burdet, M., Sutter, E., Pexieder, T., Nicod, P., and Meda, P. (2000). Connexin37 in normal and pathological development of mouse heart and great arteries. Dev. Dyn. *218*, 331–344.

Harlow, E., and Lane, D. (1988). Antibodies. A Laboratory Manual. Cold Spring Harbor: Cold Spring Harbor Laboratory Press, 726 pp.

Hong, T., and Hill, C.E. (1998). Restricted expression of the gap junctional protein connexin43 in the arterial system of the rat. J. Anat. *193*, 583–593.

Huang, G.Y., Cooper, E.S., Waldo, K., Kirby, M.L., Gilula, N.B., and Lo, C.W. (1998). Gap junction-mediated cell-cell communication modulates mouse neural crest migration. J. Cell Biol. *143*, 1725–1734.

Kumar, N., and Gilula, N.B. (1996). The gap junction communication channel. Cell *84*, 381–388.

Larson, D.M., Carson, M.P., and Haudenschild, C.C. (1987). Junctional transfer of small molecules in cultured bovine brain microvascular endothelial cells and pericytes. Microvasc. Res. *34*, 184–199.

Larson, D.M., and Haudenschild, C.C. (1988). Junctional transfer in wounded cultures of bovine aortic endothelial cells. Lab. Invest. *59*, 373–379.

Larson, D.M., Haudenschild, C.C., and Beyer, E.C. (1990). Gap junction messenger RNA expression by the vascular wall cells. Circ. Res. *66*, 1074–1080.

Larson, D.M., and Sheridan, J.D. (1982). Intercellular junctions and transfer of small molecules in primary vascular endothelial cells. J. Cell Biol. *92*, 183–191.

Little, T.L., Beyer, E.C., and Duling, B.R. (1995a). Connexin 43 and connexin 40 gap junctional proteins are present in arteriolar smooth muscle and endothelium in vivo. Am. J. Physiol. *268*, H729–H739.

Little, T.L., Yia, J., and Duling, B.R. (1995b). Dye tracers define differential endothelial and smooth muscle coupling patterns within the arteriolar wall. Circ. Res. *76*, 498–504.

Montesano, R., Pepper, M.S., Möhle-Steinlein, U., Risau, W., Wagner, E.F., and Orci, L. (1990). Increased proteolytic activity is responsible for the aberrant morphogenetic behavior of endothelial cells expressing middle T oncogene. Cell *62*, 435–445.

Paul, D.L., Yu, K., Bruzzone, R., Gimlich, R.L., and Goodenough, D.A. (1995). Expression of a dominant negative inhibitor of intercellular communication in the early *Xenopus* embryo causes delamination and extrusion of cells. Development *121*, 371–381.

Pepper, M.S., and Meda, P. (1992). Basic fibroblast growth factor increases junctional communication and connexin 43 expression in microvascular endothelial cells. J. Cell. Physiol. *153*, 196–205.

Pepper, M.S., Montesano, R., El Aoumari, A., Gros, D., Orci, L., and Meda, P. (1992). Coupling and connexin 43 expression in microvascular and large vessel endothelial cells. Am. J. Physiol. *262*, C1246–C1257.

Pepper, M.S., Spray, D.C., Chanson, M., Montesano, R., Orci, L., and Meda, P. (1989). Junctional communication is induced in migrating capillary endothelial cells. J. Cell Biol. *109*, 3027–3038.

Pepper, M.S., Tacchini-Cottier, F., Sabapathy, T.K., Montesano, R., and Wagner, E.F. (1997). Endothelial cells transformed by polyomavirus middle T oncogene: a model for hemangiomas and other vascular tumors. In: Tumor Angiogenesis, ed. R. Bicknell, C E. Lewis, and N. Ferrara, Oxford, United Kingdom: Oxford University Press, 309–331.

Reed, K.E., Westphale, E.M., Larson, D.M., Wang, H.-Z., Veenstra, R.D., and Beyer, E.C. (1993). Molecular cloning and functional expression of human connexin37, an endothelial cell gap junction protein. J. Clin. Invest. *91*, 997–1004.

Risau, W. (1991). Vasculogenesis, angiogenesis and endothelial cell differentiation during embryonic development. In: The development of the vascular system, ed. R N. Feinberg, G.K. Sherere, and R. Auerbach, Basel, Switzerland: Karger, 58–68.

Schwartz, S.M., Haudenschild, C.C., and Eddy, E.M. (1978). Endothelial regeneration. 1. Quantitative analysis of initial stages of endothelial regeneration in rat aortic intima. Lab. Invest. *38*, 568–580.

Stewart, W.W. (1978). Functional connections between cells as revealed by dye coupling with a highly fluorescent naphthalimide tracer. Cell *14*, 741–759.

Sullivan, R., and Lo, C.W. (1995). Expression of a connexin 43/b-galactosidase fusion protein inhibits gap junctional communication in NIH3T3 cells. J. Cell Biol. *130*, 419–429.

VanRijen, H.V.M., VanKempen, M.J.A., Analbers, L.J.S., Rook, M.B., VanGinneken, A.C.G., Gros, D., and Jongsma, H.J. (1997). Gap junctions in human umbilical cord endothelial cells contains multiple connexins. Am. J. Physiol. *272*, C117–C130.

Vassali, J.-D., Dayer, J.M., Wohlwend, A., and Belin, D. (1984). Concomitant secretion of prourokinase and of a plasminogen activator-specific inhibitor by cultured human monocytes-macrophages. J. Exp. Med. *159*, 1653–1668.

White, T.W., and Paul, D.L. (1999). Genetic diseases and gene knockouts reveal diverse connexin functions. Annu. Rev. Physiol. *61*, 283–310.

Yeh, H.-I., Dupont, E., Coppen, S., Rothery, S., and Severs, N.J. (1997). Gap junction localization and connexin expression in cytochemically identified endothelial cells of arterial tissue. J. Histochem. Cytochem. *45*, 539–550.